

# Monte Carlo study of the $S = \frac{1}{2}$ and $S = 1$ Heisenberg antiferromagnet on a spatially anisotropic square lattice

Y. J. Kim and R. J. Birgeneau\*

*Department of Physics, Massachusetts Institute of Technology, Cambridge, Massachusetts 02139*

(Received 18 April 2000)

We present a quantum Monte Carlo study of a Heisenberg antiferromagnet on a spatially anisotropic square lattice, where the coupling strength in the  $x$  direction ( $J_x$ ) is different from that in the  $y$  direction ( $J_y$ ). By varying the anisotropy  $\alpha$  from 0 to 1, we interpolate between the one-dimensional chain and the two-dimensional isotropic square lattice. Both  $S = 1/2$  and  $S = 1$  systems are considered separately in order to facilitate comparison. The temperature dependence of the uniform susceptibility and the spin-spin correlation length are computed down to very low temperatures for various values of  $\alpha$ . For  $S = 1$ , the existence of a quantum critical point at  $\alpha_c^{S=1} = 0.040(5)$  as well as the scaling of the spin gap is confirmed. Universal quantities predicted from the  $\mathcal{O}(3)$  nonlinear  $\sigma$  model agree with our results at  $\alpha = 0.04$  without any adjustable parameters. On the other hand, the  $S = 1/2$  results are consistent with  $\alpha_c^{S=1/2} = 0$ , as discussed by a number of previous theoretical studies. Experimental implications for  $S = 1/2$  compounds such as  $\text{Sr}_2\text{CuO}_3$  are also discussed.

## I. INTRODUCTION

Low dimensional quantum magnetism is currently one of the most intensively studied fields in condensed-matter physics. Through the synergistic efforts of theory, numerical simulation, and experiment, our understanding of the static and dynamic behavior of low dimensional quantum magnets has grown tremendously. The study of the one-dimensional (1D) quantum Heisenberg antiferromagnet (QHA) has a long history dating back to the exact solution found by Bethe<sup>1</sup> for the  $S = 1/2$  nearest-neighbor (NN) chain. He found the ground-state eigenfunction for this system and showed that there is no long-range order at  $T = 0$ , unlike its classical counterpart. The Bethe-Ansatz solution, however, is peculiar to the  $S = 1/2$  chain and cannot be readily generalized. Recent theoretical advances in quantum magnetism have come primarily from applications of quantum field theory techniques. The low-energy, long-wavelength behavior of quantum antiferromagnets can be mapped onto an effective relativistic field theory.

In his pioneering work based on the large-spin, semiclassical mapping of the 1D QHA to the  $\mathcal{O}(3)$  quantum nonlinear  $\sigma$  model (QNL $\sigma$ M) in  $(1+1)$  dimensions,<sup>2</sup> Haldane conjectured that all half-odd-integer spin chains should behave qualitatively like a  $S = 1/2$  chain, while for integer spin chains the zero-temperature spin correlations should decay exponentially with distance due to the presence of the so-called Haldane gap,  $\Delta$ . In two-dimensions, Chakravarty, Halperin, and Nelson<sup>3</sup> have mapped the long-wavelength, low-temperature behavior of the two-dimensional (2D) QHA onto the  $(2+1)$  dimensional QNL $\sigma$ M. They obtained a phase diagram for the system with three regimes: quantum disordered (QD), quantum critical (QC), and renormalized classical (RC). In the QD regime, the spin correlation length  $\xi$  remains finite even at  $T = 0$ , as in the case of the  $S = 1$  spin chain. In the QC regime, temperature is the only relevant energy scale, and thus  $\xi$  diverges like  $\sim T^{-1}$  as  $T \rightarrow 0$ :  $T$

$= 0$  is the quantum critical point. In the RC regime, the correlation length diverges exponentially [ $\sim \exp(1/T)$ ], so that the ground state has long-range order.

Due to the peculiar role played by the spin quantum number in the ground-state properties, the 1D QHA has been much studied since Haldane's conjecture. The 2D QHA has also attracted considerable attention both for its intrinsic interest and also because the magnetism in the parent compounds of the high temperature superconductors is well described by the  $S = 1/2$  2D QHA. Recently, attention has been given to the physics of magnetism in intermediate dimensions; namely, systems which exhibit a crossover from one to two dimensions. One can think of two different approaches to explore this problem. One method is to begin with spin ladders, which are obtained by coupling a small number of spin chains, and then to increase the number of chains in the spin ladder until 2D physics is obtained. Alternatively, one can begin with an infinite number of decoupled spin chains, and then increase the coupling between the spin chains gradually until the interchain coupling becomes comparable to the intrachain coupling; in other words, one studies a spatially anisotropic square lattice quantum Heisenberg antiferromagnet (SASLQHA). Spin ladders have been studied much recently, and have revealed the initially surprising result that the ground-state properties of the  $S = 1/2$  spin ladder depend on the number of chains in the ladder,<sup>4</sup> analogous to the 1D QHA. Specifically, when even numbers of chains (or legs) are coupled to form a ladder (even- $n$ ), they show the same universal behavior as integer spin chains, while odd- $n$   $S = 1/2$  ladders behave essentially like a single  $S = 1/2$  chain at low temperatures and long wavelengths.

Our study focuses on the SASLQHA, in which the dimensional parameter (interchain coupling) can be varied *continuously*. The Hamiltonian of the SASLQHA is essentially that of parallel spin chains forming a square lattice with interchain coupling  $J_x$  ( $J_x > 0$ ):

$$\mathcal{H} = J_y \sum_{i,j} \mathbf{S}_{i,j} \cdot \mathbf{S}_{i+1,j} + \sum_{i,j} J_x \mathbf{S}_{i,j} \cdot \mathbf{S}_{i,j+1}. \quad (1)$$

Here  $i$  and  $j$  label lattice sites along the  $y$  direction and the  $x$  direction, respectively. We will set  $J_y = J$  and use  $\alpha \equiv J_x/J_y$  as an anisotropy parameter in this paper. We use units in which  $\hbar = k_B = g\mu_B = 1$ , and set the lattice constant  $a = 1$  along both the  $x$  and  $y$  directions. By varying  $0 \leq \alpha \leq 1$ , the Hamiltonian Eq. (1) can interpolate between a single spin chain and an isotropic square lattice. The  $S = 1/2$  case has drawn special attention recently, due to its conjectured relevance to the physics of stripe structures in high-temperature superconductors.<sup>5,6</sup>

One of the most interesting questions in the physics of the SASLQHA is the nature of the ground state. Since the ground state of the 1D QHA ( $\alpha = 0$ ) is disordered while the QHA on an isotropic square lattice ( $\alpha = 1$ ) has a Néel ordered ground state, there should be an order-disorder quantum transition for a critical value of  $\alpha = \alpha_c$ . For  $S = 1$  this seems intuitively clear. As  $\alpha$  is increased from zero, the Haldane gap will decrease smoothly, vanishing at a nonzero  $\alpha_c^{S=1}$ . However, it is not at all obvious what the behavior should be for  $S = 1/2$ . Although it is widely believed that  $\alpha_c^{S=1/2} = 0$ , there are a few studies claiming otherwise.<sup>5,7</sup> Sakai and Takahashi<sup>8</sup> first considered the Hamiltonian Eq. (1) by treating the interchain coupling in the small  $\alpha$  limit via mean-field theory. They also estimated that  $\alpha_c^{S=1/2} \approx 0$  and  $\alpha_c^{S=1} \approx 0.025$  by calculating the susceptibility via numerical Lanczos diagonalization. Azzouz and co-workers obtained essentially the same results from their field theoretical study, albeit with smaller  $\alpha_c^{S=1} \approx 0.00186$ .<sup>9,10</sup> The renormalization-group argument by Affleck and co-workers<sup>11,12</sup> suggests that the answer is not universal but depends on the microscopic details of the model. For the nearest-neighbor model [Eq. (1)],  $\alpha_c^{S=1/2} = 0$  was shown by zero-temperature series expansions.

In this paper we show that our quantum Monte Carlo study of the  $S = 1/2$  SASLQHA gives results which are consistent with the claim that Néel order sets in for infinitesimal  $\alpha$  for  $S = 1/2$ .<sup>8,10,11,13-16</sup> For the  $S = 1$  SASLQHA, we show that  $\alpha_c^{S=1} = 0.040(5)$  is the quantum critical point; we find that the thermodynamic properties at this point follow the  $\mathcal{O}(3)$  QNL $\sigma$ M predictions remarkably well. We compare three quantities: the dimensionless ratio  $S_Q/T\chi_s$  (defined below), the temperature dependences of the correlation length  $\xi$ , and the uniform susceptibility  $\chi_u$ . These quantities agree quantitatively with the QNL $\sigma$ M values without any adjustable parameter.

We have carried out quantum Monte Carlo simulations on large lattices utilizing the loop cluster algorithm. The lattice size has been kept at least ten times larger than the calculated correlation length. The lengths and Trotter numbers of the simulated lattices are chosen so as to minimize any finite-size and lattice-spacing effects. Spin states are updated about  $2^{14}$  times to reach equilibrium and then measured  $2^{15}$  times. The same algorithm has been applied successfully in studying spin chains and spin ladders.<sup>17-19</sup> We compute the temperature ( $T$ ) and anisotropy ( $\alpha$ ) dependence of the uniform susceptibility,  $\chi_u(\alpha, T)$ ; the correlation length,  $\xi(\alpha, T)$ ; the staggered susceptibility,  $\chi_s(\alpha, T)$ ; and the static structure factor at the antiferromagnetic wave vector  $Q = (\pi, \pi)$ ,  $S_Q(\alpha, T)$  for both the  $S = 1/2$  and  $S = 1$  SASLQHA.

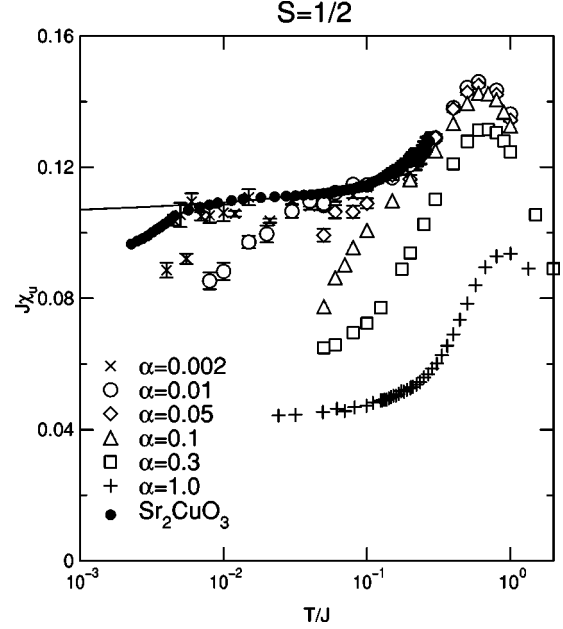


FIG. 1. The uniform susceptibility per spin,  $\chi_u$  for  $S = 1/2$ , is shown as a function of  $T$  for various  $\alpha$  in semilogarithmic scale.  $\alpha = 1$  data are taken from Ref. 20. The  $\text{Sr}_2\text{CuO}_3$  experimental results (Ref. 21) are also shown; they are scaled to fit the Monte Carlo results and  $J = 2200$  K is used to scale temperature. The solid line is a plot of the field theory result from Ref. 22.

The structure of this paper is as follows: Our Monte Carlo results for the  $S = 1/2$  SASLQHA are presented in Sec. II. The uniform susceptibility and the correlation length data are shown and discussed here. We present the  $S = 1$  SASLQHA Monte Carlo results in Sec. III. In Sec. IV, we determine and discuss the phase diagram of the  $S = 1/2$  and  $S = 1$  SASLQHA using QNL $\sigma$ M language, especially focusing on the quantum critical behavior. In Sec. V, implications of this study in relation to experiments and other related low dimensional quantum magnets are discussed.

## II. RESULTS FOR $S = 1/2$

In Fig. 1 we show the uniform susceptibility per spin for  $S = 1/2$ , as a function of  $T$  for various  $\alpha$  in semilog scale. The results for the  $\alpha = 1$  square lattice are taken from the recent Monte Carlo study by Kim and Troyer.<sup>20</sup> The crossover from 1D to 2D behavior is clear in this figure. For small  $\alpha$ , the uniform susceptibility follows that of a single chain, but begins to deviate around  $T/J \sim 5\alpha$ . For larger  $\alpha$ ,  $\chi_u$  lies intermediate between those for a single chain and the square lattice, as expected.

In the small  $\alpha$  limit, the Monte Carlo results can be compared with the results of experiments on weakly coupled spin chains. In particular,  $\text{Sr}_2\text{CuO}_3$  has a structure where  $S = 1/2$  spin chains lie along the crystallographic  $b$  direction. The interchain interaction along the  $a$  direction is frustrated, thus making this system quasi-two-dimensional. In the  $bc$  plane, the interaction along the  $c$  direction is much smaller than that in the  $b$  direction, therefore  $\text{Sr}_2\text{CuO}_3$  is a very good realization of the  $S = 1/2$  SASLQHA in the small  $\alpha$  limit. Specifically, the crystallographic  $b$  direction corresponds to the  $y$  direction in the notation of the Hamiltonian, Eq. (1), while

the  $c$  direction corresponds to the  $x$  direction. Recently Motoyama and co-workers<sup>21</sup> measured the magnetic susceptibility of  $\text{Sr}_2\text{CuO}_3$ . They extracted a value for the intrachain exchange  $J=2200(200)\text{K}$  by fitting the result to the theoretical expression proposed by Eggert *et al.*<sup>22</sup> Motoyama *et al.* also observed the logarithmic correction term predicted in the theory. However, a sudden drop in the susceptibility near 20 K was observed, and this was attributed to the onset of three-dimensional (3D) Néel order. In Fig. 1, the  $\text{Sr}_2\text{CuO}_3$  experimental results are shown as solid circles using  $J=J_b=2200\text{K}$ . As one can see from the figure, this drop can be naturally explained by a small but nonzero interchain coupling. From a comparison with our Monte Carlo results, one can estimate the interchain coupling in  $\text{Sr}_2\text{CuO}_3$  as  $J_c=J_x \approx 0.002J \approx 0.4\text{meV}$ .

A couple of points need to be mentioned in estimating the interchain coupling in  $\text{Sr}_2\text{CuO}_3$ . First, since the analysis of the susceptibility data involves the subtraction of a Curie term due to impurities, subtle effects may be difficult to interpret unambiguously. However, recent nuclear magnetic resonance Knight shift measurements, in which the Knight shift is proportional to the uniform susceptibility, show complete agreement with the susceptibility data.<sup>23</sup> Second, Schulz<sup>24</sup> and Wang<sup>25</sup> have predicted the staggered magnetization of this system as a function of the interchain coupling,  $m_0=0.72(J_\perp/J)^{1/2}$  from their interchain mean-field theory.<sup>26</sup> With  $\alpha=0.002$ , we obtain  $m_0=0.032 \approx 0.064\mu_B$ , which agrees with the experimentally<sup>27</sup> determined value of  $0.06(1)\mu_B$ , giving credence to our estimate of the interchain coupling in  $\text{Sr}_2\text{CuO}_3$ .

The spin-spin correlation length is deduced from fits of the calculated instantaneous spin-spin correlation function to the asymptotic Ornstein-Zernike (OZ) form. Only large distance numerical data are included in the fits to ensure that the asymptotic behavior is probed. As discussed in our previous Monte Carlo studies of quantum spin systems,<sup>17,18</sup> the 1D OZ form works best at high temperatures, while the 2D OZ form works better at low temperatures. However, for the  $S=1$  SASLQHA we observe a crossover to the 3D OZ form at low temperatures. This crossover of the correlation function will be discussed in Sec. V.

The correlation lengths so obtained for  $S=1/2$  are plotted in Fig. 2 on a logarithmic scale as a function of inverse temperature. Therefore linear behavior in this plot corresponds to an exponential dependence on  $T^{-1}$ , and the slope corresponds to the spin stiffness. At low enough temperatures, all data show linear behavior except for  $\alpha=0$ , signaling that  $\alpha=0$  is indeed a critical point. The solid lines are the results of fits to the crossover form suggested by Castro Neto and Hone,<sup>5</sup> which interpolates between the low- $T$  expression calculated by Hasenfratz and Niedermayer<sup>28</sup> for the  $(2+1)$ -dimensional QNL $\sigma$ M and  $\xi \sim T^{-1}$  at high temperature:

$$\xi = A \exp[2\pi\rho_s(\alpha)/T] / \left[ 1 + \frac{1}{2} \frac{T}{2\pi\rho_s(\alpha)} \right]. \quad (2)$$

Two adjustable parameters are used in the fitting:  $A$  and  $\rho_s$ . The anisotropy dependence of  $\rho_s(\alpha)$  is used to provide a crossover temperature scale between quantum critical and renormalized classical behavior in Sec. IV. We find that the

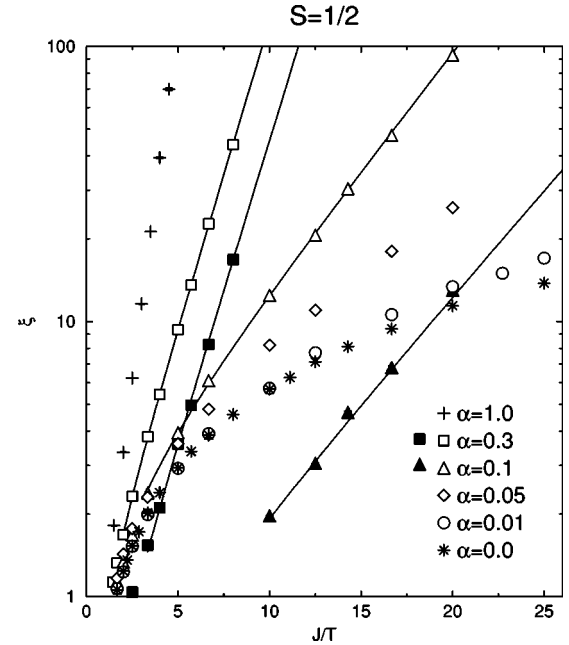


FIG. 2. The correlation length for  $S=1/2$  as a function of  $J/T$  for various values of  $\alpha$  in a logarithmic scale. Filled symbols denote the correlation length in the  $x$  direction ( $\xi_x$ ), while open symbols are  $\xi_y$  data. For small  $\alpha$  ( $\alpha \leq 0.05$ ), the  $\xi_x$ 's are smaller than one lattice constant and are not shown in the figure. Solid lines are fits to Eq. (2), showing the exponential dependence of  $\xi$  on  $T^{-1}$ .

$\rho_s(\alpha)$  values extracted from fitting  $\xi_x$  and  $\xi_y$  agree within the errors, as evidenced by the identical slopes in Fig. 2.

### III. RESULTS FOR $S=1$

The uniform susceptibility data for  $S=1$  are shown in Fig. 3. The results for the square lattice ( $\alpha=1$ ) are taken from recent QMC work by Harada and co-workers.<sup>29</sup> As in the  $S=1/2$  case, for small  $\alpha$  any deviation from the single chain data is only observed at very low temperatures. As is evident in Fig. 3, one observes distinctively different behavior for  $\alpha=0.02$  compared with that for  $\alpha=0.05$ . Specifically,  $\chi_u(\alpha=0.02)$  drops to zero at low temperatures, signaling the opening of a spin gap and concomitantly a spin liquid ground state. Indeed, one can fit the data with the asymptotic form  $\chi_u(T) \sim \exp(-\Delta/T)$  at low temperatures. The result of the fit is shown as the solid line for  $\alpha=0.02$  in Fig. 3. The spin gap values from these fits are as follows:  $\Delta(\alpha=0.01)/J=0.32(1)$ ,  $\Delta(\alpha=0.02)/J=0.25(1)$ , and  $\Delta(\alpha=0.03)/J=0.17(1)$ . Note that the  $\alpha=0.01$  and  $\alpha=0.03$  data are not shown in Fig. 3 for graphical purposes.

In Fig. 4, the correlation length data in the  $y$  direction are plotted for  $S=1$ . Since most correlation length data along the  $x$  direction are smaller than one lattice constant, they are not plotted. Note the linear scale in this figure, unlike the logarithmic scale in Fig. 2 for  $S=1/2$ . This clearly shows the  $1/T$  dependence of the correlation length for  $\alpha=0.04$ , which thus identifies  $\alpha=0.04$  as a quantum critical point. For smaller values of  $\alpha$  the correlation length saturates at low temperatures:  $\xi_0(\alpha=0.01)=7.0(2)$ ,  $\xi_0(\alpha=0.02)=10.8(5)$ ,  $\xi_0(\alpha=0.03)=19.0(5)$ . For  $\alpha > \alpha_c$ , the correlation length diverges exponentially in  $1/T$ . Therefore one can

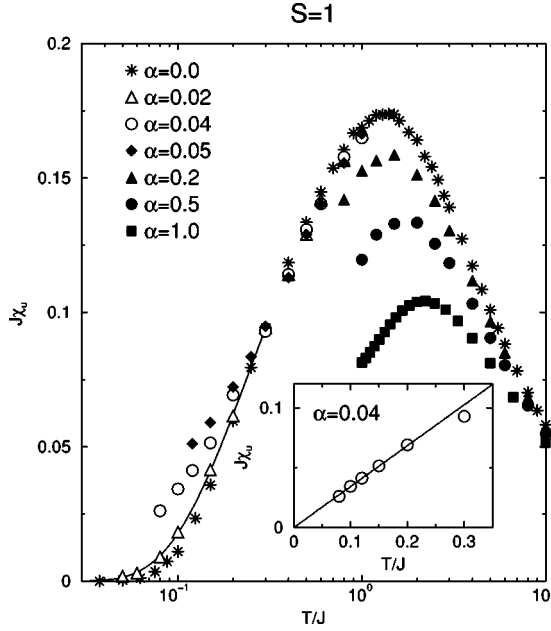


FIG. 3. The uniform susceptibility per spin,  $\chi_u$  for  $S=1$ , shown as a function of  $T$  for various values of  $\alpha$  on a semilogarithmic scale. The  $\alpha=1$  data are taken from Ref. 28. The solid line is the result of a fit to the asymptotic form  $\chi_u \sim \exp(-\Delta/T)$ . Inset: The  $\alpha=0.04$  data on a linear scale. The solid line is  $J\chi_u = 0.34T/J$ .

fit the data to Eq. (2) to obtain the spin stiffness  $\rho_s(\alpha)$ .

Some precautions are necessary in extracting the correlation length from the correlation function via fits to the OZ form. The OZ form for the correlation function in general is

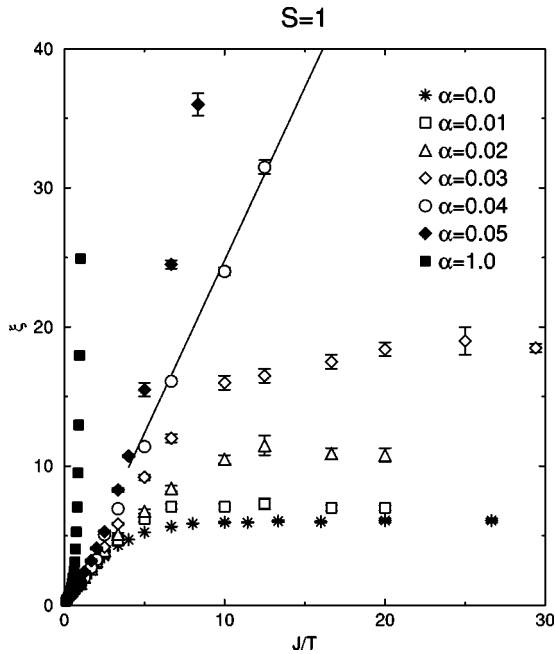


FIG. 4. The correlation length along the  $y$  direction,  $\xi_y$ , for  $S = 1$  as a function of  $J/T$  for various values of  $\alpha$ . Note that this plot is on a linear scale, so that the straight line through the  $\alpha=0.04$  data signifies the  $1/T$  dependence of  $\xi$ . Filled symbols show exponentially diverging correlation lengths, while open symbols show the saturation of the correlation length at low temperature for a QD ground state.

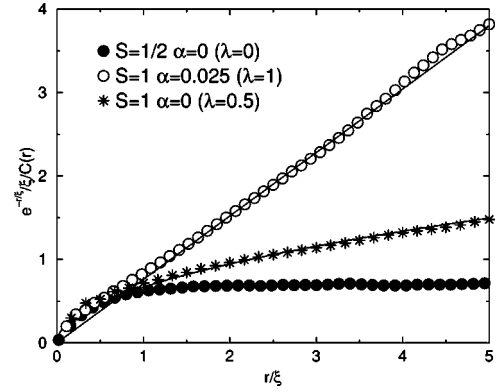


FIG. 5. Inverse correlation function multiplied by the exponential factor  $e^{-r/\xi}/\xi/C(r)$  plotted as a function of distance  $r/\xi$ . The solid lines are the results of fits to the form  $\sim r^{-\lambda}$  with  $\lambda$  fixed at the given values. All data are taken at  $T/J=0.04$ .

$$C(r) \sim \frac{e^{-r/\xi}}{r^\lambda}, \quad \lambda = \frac{(d-1)}{2}, \quad (3)$$

where  $d$  is the dimensionality. In quantum systems at low temperatures,  $d$  should be replaced by the effective dimensionality  $(d+1)$ . Since the low-temperature and long-wavelength behavior of the  $S=1$  SASLQHA with nonzero  $\alpha$  is mapped onto the  $(2+1)$ -dimensional  $\mathcal{O}(3)$  QNL $\sigma$ M, the functional form of the correlation function at low temperatures and long distances should be the OZ form with  $\lambda=1$ . Similarly, the 1D  $S=1$  spin chain (SASLQHA with  $\alpha=0$ ) has a correlation function of the  $\lambda=0.5$  OZ form.<sup>18</sup> We indeed observe a crossover in the functional form of  $C(r)$  from  $\lambda=0.5$  to  $\lambda=1$  by increasing  $\alpha$  from zero to a small but nonzero value in the  $S=1$  SASLQHA. In Fig. 5, the correlation function at the low temperature  $T/J=0.04$  is plotted to illustrate the difference in  $\lambda$ . In order to show the subtle  $\lambda$  dependence,  $1/C(r)$  is multiplied by the exponential factor, and only the  $e^{-r/\xi}/\xi/C(r) \sim r^{-\lambda}$  part is shown as a function of  $r/\xi$ . The  $\lambda=1$  behavior is apparent for  $\alpha=0.025$ , while  $\lambda=0.5$  describes the  $\alpha=0$  data better. For comparison purposes,  $C(r)$  for an  $S=1/2$  chain ( $\alpha=0$ ) is also plotted; in that case the  $\lambda=0$  behavior is quite clear.

One should note that this crossover is observed only in the QD phase, since the finite correlation lengths in this phase allow the QMC technique to probe the low-temperature behavior. On the other hand, in phases with a diverging correlation length, it is difficult to study the ground-state properties with the QMC method. Considering that the SASLQHA behaves classically at high temperatures, it is possible that the  $S=1/2$  data in Fig. 5 ( $T/J=0.04$ ) have not reached low enough temperatures to show the true ground-state behavior of  $\lambda=0.5$ . In deducing the correlation length data shown in Fig. 4, the  $\lambda=1$  form was used for  $\alpha \geq 0.02$  at low temperatures, while  $\lambda=0.5$  was used otherwise.

#### IV. QUANTUM CRITICAL POINT

The phase diagram of the  $S=1$  SASLQHA is sketched in Fig. 6, where we use the energy gap  $\Delta$  and spin stiffness  $2\pi\rho_s$ , obtained from the fits discussed in previous sections as the crossover energy scales. We use the terminology of



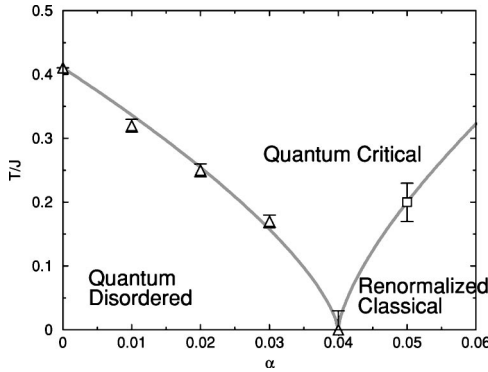


FIG. 6. Phase diagram of the  $S=1$  SASLQHA. The open squares are  $2\pi\rho_s/J$  obtained by fitting the correlation length to the asymptotic form Eq. (2), and the open triangles are the energy gap  $\Delta/J$  obtained by fitting the uniform susceptibility to the form  $\sim \exp(-\Delta/T)$ . The shaded lines are the power laws, Eqs. (4) and (5).

the  $\mathcal{O}(3)$  QNL $\sigma$ M to identify the different phases in the figure.<sup>3</sup> The inverse anisotropy ratio  $1/\alpha$  corresponds to the coupling constant  $g$ . The  $S=1/2$  phase diagram is almost identical to that of Ref. 30, and hence is not shown here.

At the quantum phase transition in  $(2+1)$  dimensions,  $\rho_s$  and  $\Delta$  obey the scaling laws

$$\rho_s \sim (g_c - g)^\nu, \quad (4)$$

$$\Delta \sim (g - g_c)^\nu, \quad (5)$$

with a critical exponent  $\nu \approx 0.69$  for the 2D QHA.<sup>31</sup> Since  $\alpha^{-1}$  plays the role of the coupling constant  $g$ , we plot  $\Delta_0(\alpha - \alpha_c)^\nu$  as a shaded line in Fig. 6. Note that  $\Delta_0$  is fixed from the  $S=1$  chain value, so that there is no adjustable parameter. The power-law scaling fits the gap data quite well, confirming that the low-temperature long-wavelength behavior of the  $S=1$  SASLQHA is consistent with that of the  $\mathcal{O}(3)$  QNL $\sigma$ M.

To illustrate that  $\alpha_c = 0.04$  is indeed the quantum critical point of the  $S=1$  SASLQHA, the dimensionless ratio  $S_Q/T\chi_s$  is plotted in Fig. 7(a). According to the QC scaling prediction for the  $\mathcal{O}(3)$  QNL $\sigma$ M,<sup>32</sup> this ratio should exhibit universal behavior in the QC regime with the specific value  $S_Q/T\chi_s = 1.10(2)$ . As shown in Fig. 7(a), the  $\alpha = 0.04$  data for  $S_Q/T\chi_s$  are constant around 1.1 at low temperatures, in quantitative agreement with the QC scaling value. This ratio has been successfully used in identifying quantum critical behavior in different systems, for example, weakly coupled spin ladders.<sup>19</sup> We also show the correlation length  $\xi_y$  multiplied by temperature in Fig. 7(b), to emphasize the  $1/T$  dependence of  $\xi_y$  at the quantum critical point,  $\alpha_c = 0.04$ , at low temperatures. Using the QNL $\sigma$ M prediction<sup>33</sup>  $\xi_y T = c/1.04$ , we obtain the spin wave velocity of  $c_y/J = 2.6$ , which is slightly larger than the 1D value (2.49), but smaller than the 2D value (3.067).

Another quantitative prediction from the  $\mathcal{O}(3)$  QNL $\sigma$ M is the uniform susceptibility. In the QC regime the uniform susceptibility is given as<sup>33</sup>

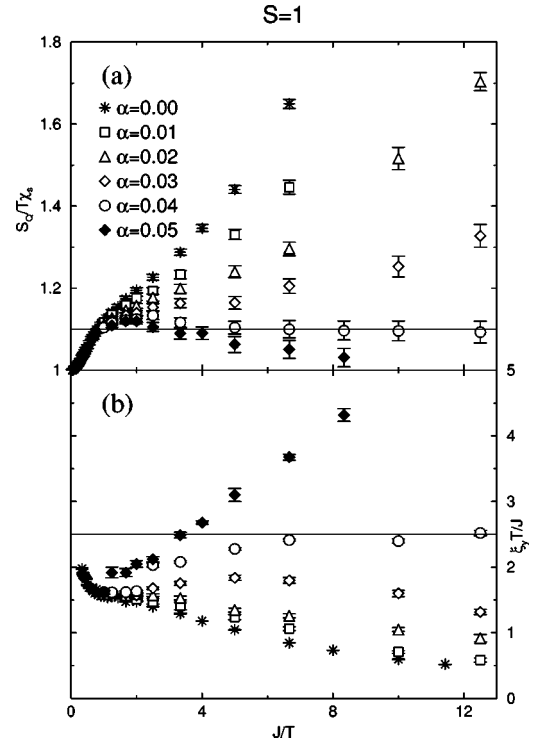


FIG. 7. (a) Dimensionless ratio  $S_Q/T\chi_s$  as a function of inverse temperature for various values of  $\alpha$ . The solid line is the prediction from the  $\mathcal{O}(3)$  QNL $\sigma$ M. (b) Correlation length multiplied by temperature as a function of inverse temperature. The solid line corresponds to the value  $c_{1D} = 2.49$ .

$$\chi_u(T) = \Omega_1(\infty) \frac{1}{c^2} T, \quad (6)$$

where  $\Omega_1(\infty) = 0.26(1)$  is a universal constant.<sup>31</sup> Since the spin-wave velocity is anisotropic in this case, one should presumably use  $c_x c_y$  instead of  $c^2$  in Eq. (6). The inset of Fig. 3 clearly shows the linear dependence of  $\chi_u$  on temperature. The fitted value of the slope is  $0.34(1)$ . Since we do not know the value of  $c_x$ , we use the fitted value of the slope and Eq. (6) to estimate  $c_x$ . If we take the spin wave velocity value  $c_y$  determined above, the spin wave velocity in the  $x$  direction is  $c_x/J \approx 0.3$ . This gives the ratio of the spin-wave velocity  $c_x/c_y \approx 0.12$ , which is very close to the value given by the series expansion study<sup>11</sup> and spin-wave theory:<sup>7</sup>  $c_x/c_y \approx 0.14$ . One should note that the anisotropy in the spin-wave velocity is enhanced from the mean-field value ( $c_x/c_y = \sqrt{\alpha} = 0.2$ ) due to quantum fluctuations.

## V. DISCUSSION

The most surprising result for the  $S=1$  SASLQHA is the smallness of the value  $\alpha_c^{S=1} \approx 0.04$ , compared with the Haldane gap value of the  $S=1$  spin chain ( $\Delta_H/J \approx 0.41$ ). One would naively think that the interchain coupling should be comparable to the Haldane gap to overcome the large energy gap and drive the system to long-range order. Indeed, such heuristic reasoning works well in the case of coupled even-legged spin ladders, where the value of the spin gap and the critical interladder coupling values are  $\sim 0.5J$  and  $\sim 0.3J$ , respectively, for an array of two-leg ladders. Corre-

sponding values for an array of four-leg ladders are  $\sim 0.1J$  and  $\sim 0.07J$ .

Recently there has been a number of studies on the nature of the ground state of  $S = 1/2$  spin ladders. Specifically, much theoretical interest has focused on the question of whether or not the ground state of the  $S = 1/2$  antiferromagnetic two-leg ladder is the same as that of the  $S = 1$  chain. Since the  $S = 1$  chain is equivalent to the  $S = 1/2$  two-leg ladder with an infinite ferromagnetic coupling, the above question can be rephrased as whether the  $S = 1/2$  ladder goes through a phase transition when the interchain coupling is varied from a positive (antiferromagnetic) value to a negative (ferromagnetic) value. White<sup>34</sup> has shown that the antiferromagnetic ladder can be transformed continuously to an  $S = 1$  chain by switching on an irrelevant next-nearest-neighbor coupling, thus claiming the equivalence of the two. Kim and co-workers<sup>35</sup> recently studied a two-leg ladder with various model parameters by a bosonization method and have provided evidence that the antiferromagnetic ladder and  $S = 1$  chain belong to different universality classes, each having distinct topological string order. Our results appear to show the distinctively different nature of the ground state of the  $S = 1$  Haldane chain and that of the antiferromagnetic ladder. However, more theoretical and numerical studies are necessary to resolve this issue unambiguously.

Although both the SASLQHA and spin ladders show crossovers between 1D and 2D behavior, the intrinsic difference between the two approaches should be noted. At high temperatures, the SASLQHA behaves as an array of decoupled chains. The 2D behavior is only observed at low temperatures, as shown in Figs. 1 and 5. However, the spin ladders at high temperatures show essentially 2D physics, since the spin-spin correlation length is shorter than the width of the spin ladder. Therefore the crossover for the spin ladders ( $2D \rightarrow 1D$  as  $T \rightarrow 0$ ) is complementary to that of the SASLQHA.

In Sec. II, we estimated the exchange interaction between chains in  $\text{Sr}_2\text{CuO}_3$  as  $\sim 0.4$  meV. Greven and Birgeneau have considered a similar exchange interaction for  $\text{SrCu}_2\text{O}_3$ .<sup>36</sup> Namely, they have noted that the effective coupling between copper spins in different ladder planes is mediated by  $\text{Sr}^{2+}$  ions and they have argued that this interladder exchange should be about 10 meV. This value is also used to describe the behavior of the three-leg ladder compound  $\text{Sr}_2\text{Cu}_3\text{O}_5$ .<sup>37</sup> This represents quite a large discrepancy between values estimated for seemingly similar superexchange interactions. However, one should observe that the geometry

of the interplane coupling in the spin ladder compound  $\text{SrCu}_2\text{O}_3$  and that of the interchain coupling in the spin chain compound  $\text{Sr}_2\text{CuO}_3$  are quite different. Specifically, in  $\text{Sr}_2\text{CuO}_3$ , all  $\text{Cu}^{2+}-\text{Sr}^{2+}-\text{Cu}^{2+}$  bond angles are close to  $90^\circ$ , while there exist linear  $\text{Cu}^{2+}-\text{Sr}^{2+}-\text{Cu}^{2+}$  bonds in  $\text{SrCu}_2\text{O}_3$  and  $\text{Sr}_2\text{Cu}_3\text{O}_5$ . If one assumes that the coupling between these  $\text{Cu}^{2+}$  ions is primarily due to the superexchange mediated by  $\text{Sr}^{2+}$  ions, one can infer that the effective interplane coupling in  $\text{SrCu}_2\text{O}_3$  is mostly due to the  $180^\circ$   $\text{Cu}^{2+}-\text{Sr}^{2+}-\text{Cu}^{2+}$  superexchange interaction. This leads us to speculate that the small value ( $\sim 0.4$  meV) of the interchain coupling in  $\text{Sr}_2\text{CuO}_3$  is due to the absence of linear  $\text{Cu}^{2+}-\text{Sr}^{2+}-\text{Cu}^{2+}$  superexchange paths.

This realization is important in understanding the spin fluctuations in superconducting  $\text{YBa}_2\text{Cu}_3\text{O}_{6+\delta}$ , since the bilayer coupling path in  $\text{YBa}_2\text{Cu}_3\text{O}_{6+\delta}$  is similar to the interplane coupling path in the spin ladder compound  $\text{SrCu}_2\text{O}_3$ .<sup>38</sup> Although the detailed nature of the hopping integral between bilayers is not known, Andersen *et al.* have shown that the hopping mediated by the yttrium ion contributes significantly to the bilayer exchange coupling.<sup>39</sup> Obviously, more theoretical calculations of the bilayer exchange interaction are needed.

In summary, we have studied the  $S = 1/2$  and  $S = 1$  SASLQHA with the quantum Monte Carlo method. By varying the anisotropy  $\alpha$  from 0 to 1, we go continuously from the one-dimensional chain to the two-dimensional isotropic square lattice. The temperature dependence of the uniform susceptibility and the spin-spin correlation length are presented for various values of  $\alpha$ . For  $S = 1$ , we show that there exists a quantum critical point at  $\alpha_c^{S=1} = 0.040(5)$ , in agreement with other analytic predictions. The power-law behavior of the spin gap is also confirmed. In addition, universal quantities predicted from the QNL $\sigma$ M, such as  $S_Q/T\chi_s \approx 1.1$  and  $\Omega_1(\infty) \approx 0.26$ , agree with our results at  $\alpha = 0.04$ , without any adjustable parameter. The  $S = 1/2$  results are consistent with  $\alpha_c^{S=1/2} = 0$ , as discussed by a number of previous theoretical studies. We also estimate the interchain coupling in the  $S = 1/2$  compound  $\text{Sr}_2\text{CuO}_3$  by comparing the measured uniform susceptibility data with our QMC results.

## ACKNOWLEDGMENTS

We would like to thank M. Greven for invaluable discussions. This work was supported by the National Science Foundation-Low Temperature Physics Programs under Grant No. DMR 97-15315.

\*Also at the Department of Physics, University of Toronto, 60 St. George Street, Toronto, Ontario M5S 1A7, Canada.

<sup>1</sup>H.A. Bethe, *Z. Phys.* **71**, 205 (1931).

<sup>2</sup>F.D.M. Haldane, *Phys. Lett.* **93A**, 464 (1983).

<sup>3</sup>S. Chakravarty, B.I. Halperin, and D.R. Nelson, *Phys. Rev. B* **39**, 2344 (1989).

<sup>4</sup>E. Dagotto and T.M. Rice, *Science* **271**, 618 (1996).

<sup>5</sup>A.H. Castro Neto and D. Hone, *Phys. Rev. Lett.* **76**, 2165 (1996).

<sup>6</sup>C.N.A. van Duin and J. Zaanen, *Phys. Rev. Lett.* **80**, 1513 (1998).

<sup>7</sup>A. Parola, S. Sorella, and Q.F. Zhong, *Phys. Rev. Lett.* **71**, 4393 (1993).

<sup>8</sup>T. Sakai and M. Takahashi, *J. Phys. Soc. Jpn.* **58**, 3131 (1989).

<sup>9</sup>M. Azzouz and B. Douçot, *Phys. Rev. B* **47**, 8660 (1993).

<sup>10</sup>M. Azzouz, *Phys. Rev. B* **48**, 6136 (1993).

<sup>11</sup>I. Affleck, M.P. Gelfand, and R.R.P. Singh, *J. Phys. A* **27**, 7313 (1994).

<sup>12</sup>I. Affleck and B.I. Halperin, *J. Phys. A* **29**, 2627 (1996).

<sup>13</sup>T. Miyazaki, D. Yoshioka, and M. Ogata, *Phys. Rev. B* **51**, 2966 (1995).

<sup>14</sup>T. Aoki, *J. Phys. Soc. Jpn.* **64**, 605 (1995).

<sup>15</sup>B. Hao and C. Gong, *Phys. Rev. B* **52**, 299 (1995).

<sup>16</sup>A.W. Sandvik, *Phys. Rev. Lett.* **83**, 3069 (1999).

<sup>17</sup>M. Greven, R.J. Birgeneau, and U.-J. Wiese, *Phys. Rev. Lett.* **77**, 1865 (1996).

- <sup>18</sup>Y.J. Kim, M. Greven, U.-J. Wiese, and R.J. Birgeneau, *Eur. Phys. J. B* **4**, 291 (1998).
- <sup>19</sup>Y.J. Kim, R.J. Birgeneau, M.A. Kastner, Y.S. Lee, Y. Endoh, G. Shirane, and K. Yamada, *Phys. Rev. B* **60**, 3294 (1999).
- <sup>20</sup>J.K. Kim and M. Troyer, *Phys. Rev. Lett.* **80**, 2705 (1998).
- <sup>21</sup>N. Motoyama, H. Esaki, and S. Uchida, *Phys. Rev. Lett.* **76**, 3212 (1996).
- <sup>22</sup>S. Eggert, I. Affleck, and M. Takahashi, *Phys. Rev. Lett.* **73**, 332 (1994).
- <sup>23</sup>K. R. Thurber (private communications).
- <sup>24</sup>H. Schulz, *Phys. Rev. Lett.* **77**, 2790 (1996).
- <sup>25</sup>Z. Wang, *Phys. Rev. Lett.* **78**, 126 (1997).
- <sup>26</sup>In Ref. 16, Sandvik has obtained logarithmic correction to the simple mean-field behavior.
- <sup>27</sup>K.M. Kojima, Y. Fudamoto, M. Larkin, G.M. Luke, J. Merrin, B. Nachumi, Y.J. Uemura, N. Motoyama, H. Eisaki, S. Uchida, K. Yamada, Y. Endoh, S. Hosoya, B.J. Sternlieb, and G. Shirane, *Phys. Rev. Lett.* **78**, 1787 (1997).
- <sup>28</sup>P. Hasenfratz and F. Niedermayer, *Phys. Lett. B* **268**, 231 (1991).
- <sup>29</sup>K. Harada, M. Troyer, and N. Kawashima, *J. Phys. Soc. Jpn.* **67**, 1130 (1998).
- <sup>30</sup>J. Tworzydło, Y. Osman, C.N.A. van Duin, and J. Zaanen, *Phys. Rev. B* **59**, 115 (1999).
- <sup>31</sup>M. Troyer, M. Imada, and K. Ueda, *J. Phys. Soc. Jpn.* **66**, 2957 (1997).
- <sup>32</sup>A. Sokol, R.L. Glenister, and R.R.P. Singh, *Phys. Rev. Lett.* **72**, 1549 (1994).
- <sup>33</sup>A.V. Chubukov, S. Sachdev, and J. Ye, *Phys. Rev. B* **49**, 11 919 (1994).
- <sup>34</sup>S.R. White, *Phys. Rev. B* **53**, 52 (1996).
- <sup>35</sup>E.H. Kim, G. Fáth, J. Sólyom, and D.J. Scalapino, cond-mat/9910023 (unpublished).
- <sup>36</sup>M. Greven and R.J. Birgeneau, *Phys. Rev. Lett.* **81**, 1945 (1998).
- <sup>37</sup>K.R. Thurber, T. Imai, T. Saitoh, M. Azuma, M. Takano, and F.C. Chou, *Phys. Rev. Lett.* **84**, 558 (2000).
- <sup>38</sup>D. Reznik, P. Bourges, H.F. Fong, L. Regnault, J. Bossy, C. Vetter, D.L. Milius, I.A. Aksay, and B. Keimer, *Phys. Rev. B* **53**, R14 741 (1996).
- <sup>39</sup>O.K. Andersen, A.I. Liechtenstein, O. Jepsen, and F. Paulsen, *J. Phys. Chem. Solids* **56**, 1573 (1995).